

Axial Chirality in 1,4-Disubstituted (ZZ)-1,3-Dienes. Surprisingly Low Energies of Activation for the Enantiomerization in Synthetically Useful Fluxional Molecules

Sandra Warren, Albert Chow, Gideon Fraenkel, and T. V. RajanBabu*

Contribution from the Department of Chemistry, The Ohio State University,
100 W. 18th Avenue, Columbus, Ohio 43210

Received March 13, 2003; E-mail: rajanbabu.1@osu.edu

Abstract: Trialkylsilyltrialkylstannes ($R_3Si-SnR'_3$) add to 1,6-diyne in the presence of Pd(0) and tris-pentafluorophenylphosphine to give 1,2-dialkylidenecyclopentanes with terminal silicon and tin substituents. The (ZZ)-geometry of these *s-cis*-1,3-dienes, resulting from the organometallic reaction mechanisms involved, forces the silicon and tin groups to be nonplanar, thus making the molecules axially chiral. There is rapid equilibration between the two helical forms at room-temperature irrespective of the size of the Si and Sn substituents. However, the two forms can be observed by 1H , ^{13}C , and ^{119}Sn NMR spectroscopy at low temperature. The rates of enantiomerization, which depend on the Si and Sn substituents, and the substitution pattern of the cyclopentane ring can be studied by dynamic NMR spectroscopy using line shape analysis. The surprisingly low energies of activation ($\Delta G^\ddagger = 52-57 \text{ kJ mol}^{-1}$) for even the bulky Si and Sn derivatives may be attributed to a widening of the exo-cyclic bond-angles of the diene carbons.

Introduction

Chirality incident in molecules with restricted rotation around a single bond, commonly referred to as axial chirality, plays an important role in the recognition events that lead to the biological activity of many natural products.¹ In asymmetric catalysis using metal complexes of biaryl ligands such as 1,1'-binaphthyl derivatives, the origin of enantioselectivity relies on this phenomenon.² Although most synthetic applications of axial chirality reported to date involve biaryl molecules, studies on other systems, especially amides with restricted rotation, are beginning to appear in the literature.³ Other molecules of this class which received early scrutiny were the highly substituted 1,3-dienes. In 1967, Boer et al. reported⁴ that hindered rotation around the 2,3-bond in a 1,3-diene was frozen by intramolecular interaction between an electrophilic Sn and an appropriately placed Br (Figure 1, 1). Later, Köbrich demonstrated that barrier to rotation (ΔG^\ddagger) in hexasubstituted 1,3-butadienes such as 2,3-dihalo-1,4-tetraphenyl-1,3-butadiene vary with the size of the halogen (Figure 1, 2a~2d).⁵ Isolation of optically active acyclic⁶ and cyclic⁷

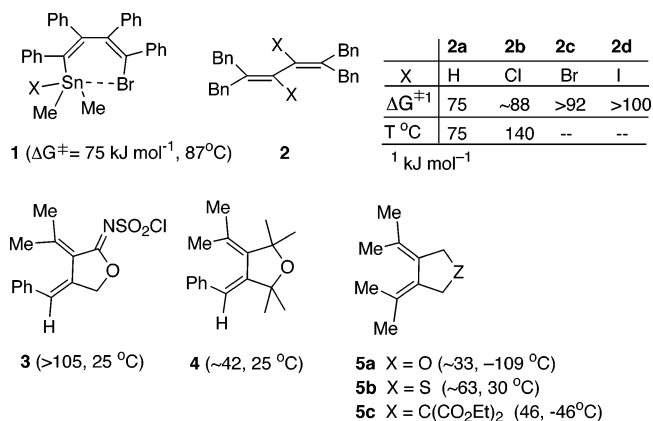
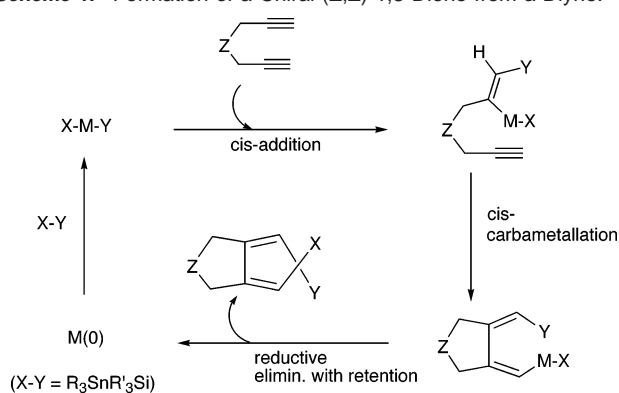


Figure 1. Axially Chiral Dienes (Activation energies, ΔG^\ddagger , are shown in brackets, kJ mol^{-1}).

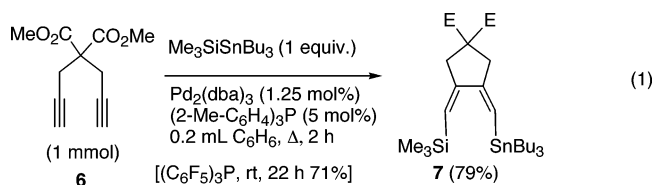
dissymmetric dienes have also been reported. Free energies of activation for enantiomerization in dissymmetric 1,2-bis-alkylidenecycloalkane derivatives have been determined by NMR methods, and these results indicate a subtle relationship between the ring substituents and the activation parameters. For example, the ΔG^\ddagger for the *N*-chlorosulfonyl imine **3**⁷ is above 105 kJ mol^{-1} , whereas the related compound **4**⁸ undergoes facile isomerization at room temperature ($\Delta G^\ddagger = 42 \text{ kJ mol}^{-1}$). The presence of heteroatoms (e.g., **5a**, **5b**) in the ring⁸ and size of the ring⁹ also have profound effects on the rates of these processes.

- (1) For two recent reviews, see: (a) Lloyd-Williams, P.; Giralt, E. *Chem. Soc. Rev.* **2001**, *30*, 145. (b) Bringmann, G.; Breuning, M.; Tasler, S. *Synthesis* **1999**, 525.
- (2) Ojima, I., Ed. *Catalytic Asymmetric Synthesis*, 2nd ed.; Wiley-VCH: New York, 2000. (b) Jacobsen, E. N.; Pfaltz, A.; Yamamoto, H., Eds.; *Comprehensive Asymmetric Catalysis*; Springer-Verlag: Berlin, 1999.
- (3) (a) Eliel, E. L.; Wilen, S. H. *Stereochemistry of Organic Compounds*; Wiley: New York, 1994, pp 1142–1166. For recent examples see, (b) Kitagawa, O.; Izawa, H.; Sato, K.; Dobashi, A.; Taguchi, T. *J. Org. Chem.* **1998**, *63*, 2634. (c) Clyden, J. *Synlett* **1998**, 810. (d) Curran, D. P.; Hale, G. R.; Geib, S. J.; Balog, A.; Cass, Q. B.; Degani, A. L. G.; Hermandes, M. Z.; Freitas, L. C. G. *Tetrahedron: Asymmetry* **1997**, *8*, 3955. (e) Godfrey, C. R. A.; Simpkins, N. S.; Walker, M. D. *Synlett* **2000**, 388. (f) Rios, R.; Jimeno, C.; Carroll, P. J.; Walsh, P. J. *J. Am. Chem. Soc.* **2002**, *124*, 10 272.
- (4) Boer, F. P.; Doorakian, G. A.; Freedman, H. H.; McKinley, S. V. *J. Am. Chem. Soc.* **1970**, *92*, 1225. For a preliminary report, see, Boer, F. P.; Flynn, J. J.; Freedman, H. H.; McKinley, S. V.; Sandel, V. R. *J. Am. Chem. Soc.* **1967**, *89*, 5068.

- (5) Köbrich, G.; Mannschreck, A.; Misra, R. A.; Rissmann, G.; Rösner, M.; Zündorf, W. *Chem. Ber.* **1972**, *105*, 3794. See also, Köbrich, G.; Kolb, B.; Mannschreck, A.; Misra, R. A. *Chem. Ber.* **1973**, *106*, 1601.; Mannschreck, A.; Jonas, V.; Bödecker, H.-O.; Elbe, H.-L.; Köbrich, G. *Tetrahedron Lett.* **1974**, 2153.; For another example, see, Bomse, D. S.; Morton, T. H. *Tetrahedron Lett.* **1974**, 3491.
- (6) Rösner, M.; Köbrich, G. *Angew. Chem., Int. Ed. Engl.* **1974**, *13*, 741.
- (7) Pasto, D. J.; Borchardt, J. K. *J. Am. Chem. Soc.* **1974**, *96*, 6220.
- (8) Jelinski, L. W.; Kiefer, E. F. *J. Am. Chem. Soc.* **1976**, *98*, 281.

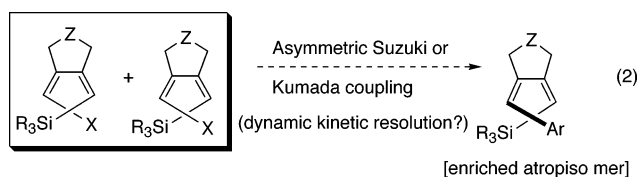
Scheme 1. Formation of a Chiral (Z,Z)-1,3-Diene from a Diyne.

Although the studies reported in the previous paragraph amply validated the concept of axial chirality in appropriately substituted 1,3-dienes, it is difficult to envisage further synthetic applications of this structural feature in these molecules because of the recalcitrant nature of the substituents in these molecules. Recently, we reported a facile synthesis of a new class of 1,4-disubstituted (Z,Z)-1,3-dienes via Pd(0)-catalyzed silyl-stannylation/cyclization of 1,6-diyne mediated by $R_3SiSnR'_3$ (eq 1).¹⁰

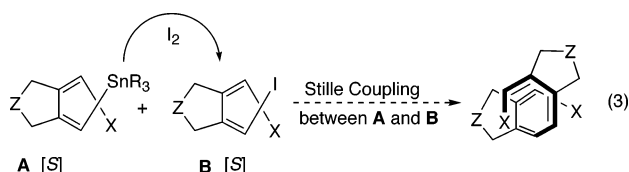


The exceptional regio- and stereochemical control arising as a necessary consequence of the organometallic mechanisms involved (Scheme 1), results in the placement of the Si and Sn substituents in an “inside” orientation, thus creating a helical motif. We expected the enantiomerization process in these systems to depend on the size of the groups on Si and Sn, and the substitution pattern around the ring.

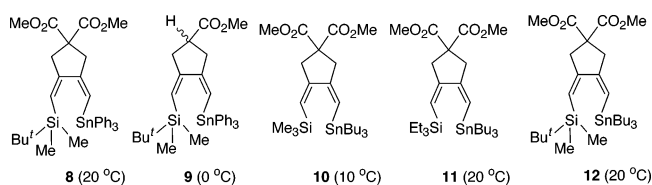
As myriad possibilities for further functionalization via the vinylsilane and vinylstannane moieties can be envisioned, these fluxional molecules are potentially valuable intermediates for stereoselective synthesis of carbocyclic and heterocyclic compounds. Among the possibilities are dynamic kinetic resolution of the dienes by reactions with suitable chiral reagents or those mediated by asymmetric catalysts (e.g., eq 2) and construction



of extended helical polyolefins (eq 3). Before contemplating



such applications, it is important to establish the relevant thermodynamic and kinetic parameters that govern this isomer-

**Figure 2.** Axially Chiral Dienes Used for Dynamic NMR Study (Approximate coalescence temperature T_c are shown in brackets).

ization process. In this context, identification of the structural features of the diene that might produce a higher barrier would also be useful. With these goals in mind, we have examined the helix inversion process by temperature-dependent dynamic NMR spectroscopy. The details are reported in this paper.

Results and Discussion

Synthesis and Characterization of the Dienes. The 1,4-silyl stannyl dienes **8**–**12** (Figure 2) were synthesized using the procedure reported earlier (eq 1).¹⁰ In each case, the structure of the compound, including the configuration of the double bond, was unambiguously established by 1H , ^{13}C , ^{119}Sn NMR spectroscopy.¹¹ The data for **8** is typical. The 1H NMR (500 MHz, $CDCl_3$, 25 °C) is characterized by the following peaks: δ – 0.70 – + 0.20 (6 H, br, $SiCH_3$), 0.78 (9 H, s, $SiCCH_3$), 3.01 (2 H, br, s, H_2), 3.20 (2 H, br, s, H_5), 3.77 (6 H, s, OCH_3), 5.23 (1 H, s, $SiCH$), 6.13 (1 H, s, $J_{HSn} = 66.4$ Hz, $SnCH$), 7.39–7.40 (9 H, m, aromatic), 7.47–7.70 (6 H, m, aromatic). Irradiation of the olefinic signal at δ 5.23 causes the enhancement of the broad peak centered around 3.01 (4.5%) and irradiation of the δ 6.13 peak causes the enhancement (5.5%) of the broad peak at δ 3.20. The broad singlets due to the C-2 and C-5 methylene protons become sharp at 105 °C (toluene- d_8). Upon cooling to –49 °C, these signals evolve into two sets of AB quartets. Likewise, the extraordinarily broad $Si[CH_3]_2$ signals (half-width at room temperature > 100 Hz) gives a clear indication of the possible fluxional nature of this molecule. Upon warming to 105 °C (toluene- d_8), this broad signal transforms into a sharp singlet, whereas upon cooling to –49 °C two sharp singlets emerge in the place of the broad peak. The corresponding ^{13}C signal is barely visible above the baseline (half-width > 400 Hz) at 25 °C between δ –5.5 to –3.5; but is a sharp singlet at 105 °C (toluene- d_8) and a set of two singlets at δ –2.5 and –5.5 at –60 °C. The other nonaromatic signals in the ^{13}C spectra ($CDCl_3$, 125 MHz) are at 17.4 (s, $SiCCH_3$), 26.3 (q, $SiCCH_3$), 43.8 (t, CH_2), 44.4 (t, CH_2), 52.9 (q, OCH_3), 54.7 (s, C_1), 122.4 (d, $SnCH$), 125.4 (d, $SiCH$), and 172.0 (s, CO). The OCH_3 and CO signals in the proton-decoupled ^{13}C spectrum split into two equally sized peaks upon cooling to –60 °C.¹¹ The ^{119}Sn peak appears at δ –154.5 ($CDCl_3$, 185 MHz). The temperature dependence of the spectrum is completely reversible. Barring a highly unlikely conformational equilibrium involving the cyclopentane ring, these changes are best explained by the axial chirality of the molecule. Molecules **9**–**12** were similarly characterized.¹¹ Hydrogen-1, carbon-13, and tin-119 NMR spectra of these compounds recorded (at 500, 125, and 185 MHz respectively) at various temperatures are included in the Supporting Information.

(9) Pasto, D. J.; Scheidt, W. R. *J. Org. Chem.* **1975**, *40*, 1444.
 (10) Gréau, S.; Radetich, B.; RajanBabu, T. V. *J. Am. Chem. Soc.* **2000**, *122*, 8579.
 (11) (a) See the Supporting Information for details and spectra. (b) Graphical representations of the temperature dependence of chemical shifts of the relevant protons are included in the Supporting Information.

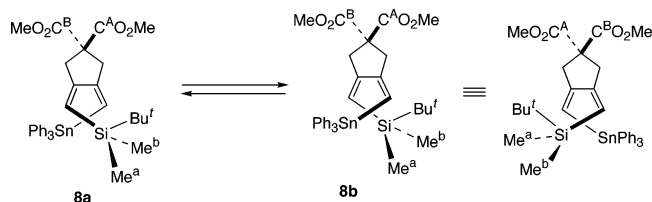


Figure 3. Exchange of the Diastereotopic Me_2Si Groups in **8** upon Inversion.

To estimate the kinetic parameters for this fast exchanging system, NMR line shape analysis as described by Kaplan and Fraenkel,¹² was employed. In the present situation, this method is almost ideal for two reasons: (a) the temperature dependence of the NMR spectra of the dienes over a wide, readily accessible range is highly reproducible, and, (b) our synthetic method makes it possible to systematically change the steric demands of the “inside” substituents. It is also possible to vary the size and the substitution pattern of the ring. Because several well-behaved spin systems undergoing exchange can be readily identified, the line shape analysis provides the one of the most accurate means for the determination of kinetic parameters for this process at equilibrium.

Line Shape Analysis. The first system studied is shown in Figure 3. Since the diene system is chiral, the two methylsilyl groups are diastereotopic and appear as two singlets in the NMR spectrum at temperatures below $-5\text{ }^\circ\text{C}$ (Figure 4). As the temperature increases, the shift between the two silyl methyls progressively averages and the peaks appear as a singlet above $\sim 28\text{ }^\circ\text{C}$. For line shape analysis purposes, this resonance can be treated as an uncoupled, equally populated, two pseudo-half spin exchanging system. The ^1H pseudo spins are labeled as A and B.



The absorption is obtained from eq 5

$$\text{Abs}(\nu) = -\text{Im}(\rho_1 + \rho_2) \quad (5)$$

where

$$\rho_1 = \langle \alpha / \rho^A / \beta \rangle, \rho_2 = \langle \alpha / \rho^B / \beta \rangle$$

The two elements (ρ_1 and ρ_2) of the density matrix are obtained by solving the two coupled equations, shown in the matrix form in eq 6.

$$\begin{bmatrix} i2\pi(\Delta\nu_a) - T^{-1} & -k & k \\ k & i2\pi(\Delta\nu_b) - T^{-1} - k & 0 \end{bmatrix} \begin{bmatrix} \rho_1 \\ \rho_2 \end{bmatrix} = iC \begin{bmatrix} 1 \\ 1 \end{bmatrix} \quad (6)$$

where $\Delta\nu_i = \nu - \nu_i$, ν_i being the frequency of species i and ν is the frequency axis of the spectrum, T^{-1} is the intrinsic line-width, C is an arbitrary constant, and k is the first-order rate constant of the exchange process. The line width used in this instance was $T^{-1} = 1.5\text{ s}^{-1}$. In this system, the shift between A and B varies in a linear fashion with temperature. Shifts over the temperature range of the study could be estimated by linear extrapolation^{11b} from the region where direct measurement was

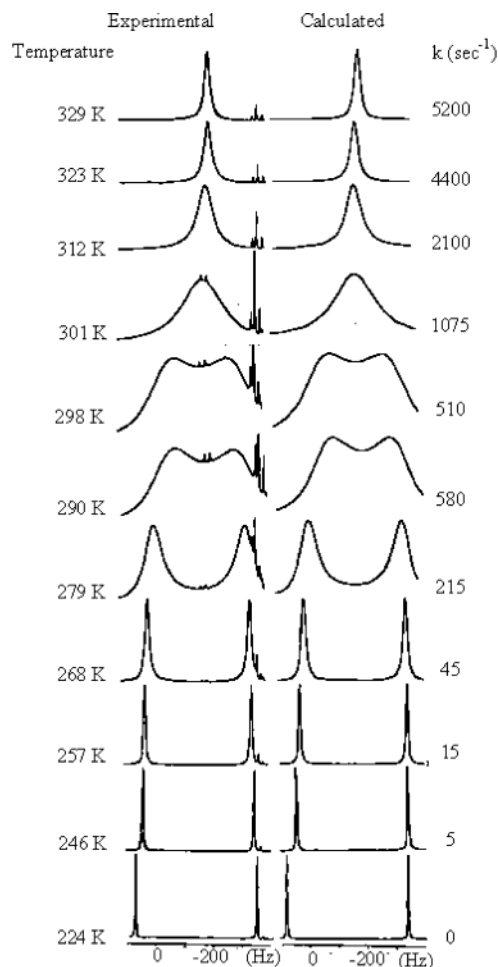


Figure 4. Experimental (left) and calculated (right) ^1H NMR line shapes due to methylsilyl groups of **8** at different temperatures with derived rate constants.

possible using the relation

$$(\nu_A - \nu_B = -1.6616T + 805.54, R^2 = 0.9987)$$

Comparisons of the observed with the calculated ^1H NMR spectra (Figure 4) provided the rate constants of the exchange process at each temperature. The Eyring plot (Figure 5) then gave the values of ΔH^\ddagger and ΔS^\ddagger ($55.4 \pm 2.2\text{ kJ}\cdot\text{mol}^{-1}$ and $-4.3 \pm 7.6\text{ J}\cdot\text{mol}^{-1}\cdot\text{K}^{-1}$ respectively).

The second system is depicted in Figure 6. The compound **9** consists of two diastereomers, with each pair of diastereotopic gem-dimethyls giving rise to two lines. The ratio of the diastereomers appear to be 1:1 from all spectral data. As the temperature increases, they average to 2 lines with some overlap between them. This system can be treated as the sum of two independent uncoupled, equally populated, two pseudo-half spin exchanging systems.



The absorption is obtained from eq 8

$$\text{Abs}(\nu) = -\text{Im}(\rho_1 + \rho_2 + \rho_3 + \rho_4) \quad (8)$$

where

$$\rho_1 = \langle \alpha / \rho^A / \beta \rangle, \rho_2 = \langle \alpha / \rho^B / \beta \rangle, \rho_3 = \langle \alpha / \rho^{A'} / \beta \rangle, \rho_4 = \langle \alpha / \rho^{B'} / \beta \rangle$$

(12) Kaplan, J. I.; Fraenkel, G. *NMR of Chemically Exchanging Systems*; Academic Press: New York, 1980.

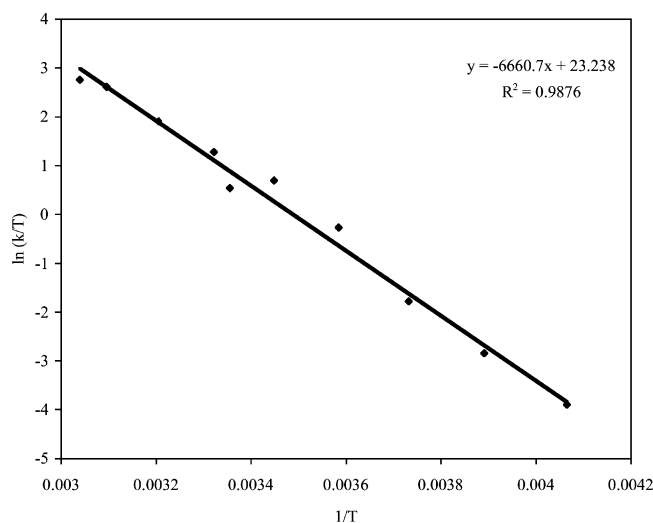


Figure 5. Eyring plot for inversion of **8** using the lineshapes of the methylsilyl resonances.

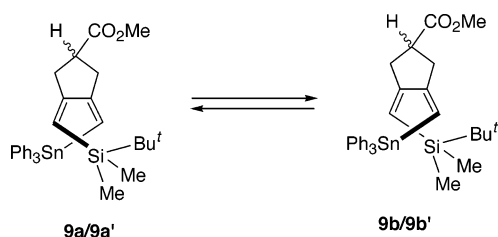


Figure 6. Exchange of the diastereotopic Me₂Si groups in **9**.

The four elements of the density matrix are obtained by solving the four coupled equations, shown in matrix form in eq 9. A line width of 3.4 Hz was used. In this case, there are two options

$$\begin{bmatrix} i2\pi(\Delta\nu_a)T^{-1}-k & k & 0 & 0 \\ k & i2\pi(\Delta\nu_b)T^{-1}-k & 0 & 0 \\ 0 & 0 & i2\pi(\Delta\nu_a)T^{-1}-k & k \\ 0 & 0 & k & i2\pi(\Delta\nu_b)T^{-1}-k \end{bmatrix} \begin{bmatrix} \rho_1 \\ \rho_2 \\ \rho_3 \\ \rho_4 \end{bmatrix} = iC \begin{bmatrix} 1 \\ 1 \\ 1 \\ 1 \end{bmatrix} \quad (9)$$

for the exchange, the first and third peaks average; the second and fourth peaks average or the first and fourth peaks average and the second and third peaks average. Both possibilities were tested and yielded the same results. Again, shift differences vary with temperature, but we were able to obtain linear correlations^{11b} between the shift differences and the temperature as follows

$$\nu_A - \nu_B = -1.8154T + 866.65, R^2 = 0.9994$$

$$\nu_{A'} - \nu_{B'} = -1.7309T + 835.89, R^2 = 0.9992$$

$$\nu_A - \nu_{A'} = -0.136T + 47.308, R^2 = 0.999$$

Comparisons of observed and calculated ¹H NMR line shapes are shown in Figure 7. The Eyring plot (Figure 8) then gives the values of ΔH^\ddagger and ΔS^\ddagger as $48.8 \pm 1.1 \text{ kJ mol}^{-1}$ and $-11.6 \pm 3.8 \text{ J mol}^{-1}\text{K}^{-1}$, respectively.

The last two systems studied are shown in Figures 9 and 10. The mathematical treatments of both systems are identical. Both

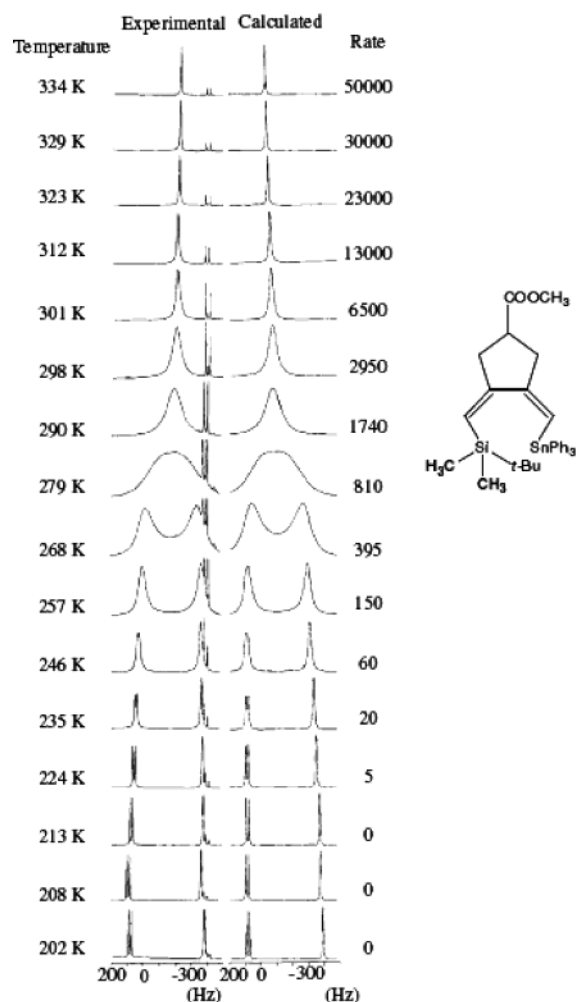


Figure 7. Experimental (left) and calculated (right) ¹H NMR line shapes due to methylsilyl groups of **9** at different temperatures with derived rate constants.

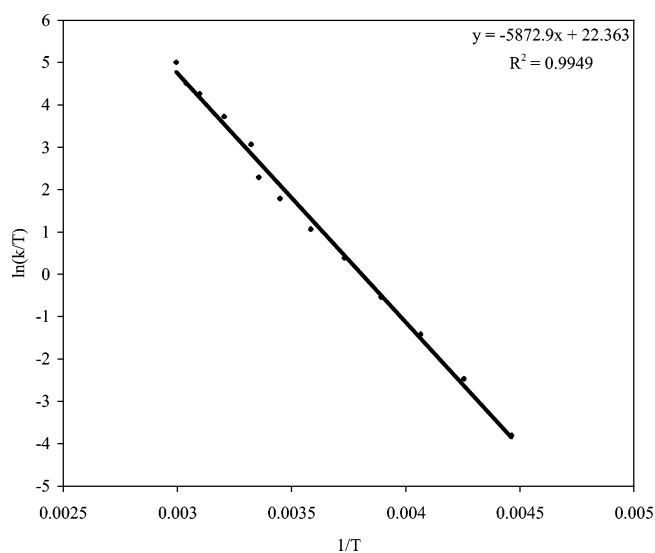


Figure 8. Eyring plot for the inversion in **9** using the line shapes of the methylsilyl resonances in ¹H NMR.

have diastereotopic methylene groups, giving rise to two AB systems. As the temperature increases, the shift between A and B averages and the methylene hydrogens eventually appear as two singlets. These systems can be treated as the sum of two

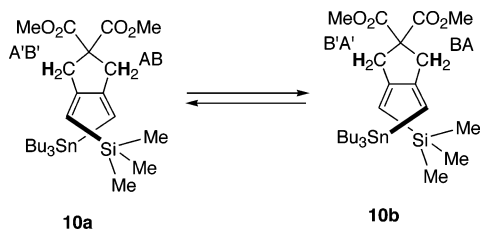


Figure 9. Inversion in 10.

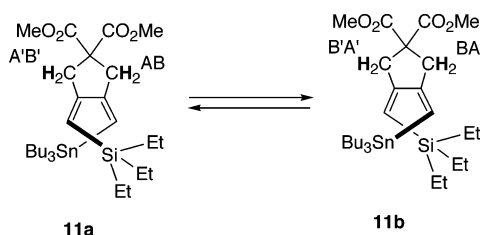


Figure 10. Inversion in 11.

independent coupled, equally populated, two-half-spin exchanging systems.



m The absorption is obtained from eq 11.

$$\text{Abs}(\nu) = -\text{Im}(\rho_1 + \rho_2 + \rho_3 + \rho_4 + \rho_5 + \rho_6 + \rho_7 + \rho_8) \quad (11)$$

where

$$\begin{aligned} \rho_1 &= \langle \alpha\alpha/\rho^{AB}/\beta\alpha \rangle, \rho_2 = \langle \alpha\beta/\rho^{AB}/\beta\beta \rangle, \rho_3 = \\ &\langle \alpha\alpha/\rho^{AB}/\alpha\beta \rangle, \rho_4 = \langle \beta\alpha/\rho^{AB}/\beta\beta \rangle, \rho_5 = \langle \alpha\alpha/\rho^{A'B'}/\beta\alpha \rangle, \rho_6 = \\ &\langle \alpha\beta/\rho^{A'B'}/\beta\beta \rangle, \rho_7 = \langle \alpha\alpha/\rho^{A'B'}/\alpha\beta \rangle, \rho_8 = \langle \beta\alpha/\rho^{A'B'}/\beta\beta \rangle \end{aligned}$$

The values of these elements of the density matrix are obtained by solving the eight coupled density matrix equation, shown in matrix form in eq 12, where J and J' are the coupling constants between H_A and H_B of the two AB systems.

In the case depicted in Figure 9, the AB shift differences vary linearly with temperature. Shifts in the exchange regime are estimated by extrapolation as before using the following

$$\begin{bmatrix} i2\pi(\Delta\nu_a - J)/2 - T^{-1} - k & 0 & i2\pi J/2 + k & 0 & 0 & 0 & 0 & 0 \\ 0 & i2\pi(\Delta\nu_a + J)/2 - T^{-1} - k & 0 & -i2\pi J/2 + k & 0 & 0 & 0 & 0 \\ i2\pi J/2 + k & 0 & i2\pi(\Delta\nu_b - J)/2 - T^{-1} - k & 0 & 0 & 0 & 0 & 0 \\ 0 & -i2\pi J/2 + k & 0 & i2\pi(\Delta\nu_b + J)/2 - T^{-1} - k & 0 & 0 & 0 & 0 \\ 0 & 0 & 0 & 0 & i2\pi(\Delta\nu_a - J')/2 - T^{-1} - k & 0 & i2\pi J'/2 + k & 0 \\ 0 & 0 & 0 & 0 & 0 & i2\pi(\Delta\nu_a + J')/2 - T^{-1} - k & 0 & -i2\pi J'/2 + k \\ 0 & 0 & 0 & 0 & i2\pi J'/2 + k & 0 & i2\pi(\Delta\nu_b - J')/2 - T^{-1} - k & 0 \\ 0 & 0 & 0 & 0 & 0 & -i2\pi J'/2 + k & 0 & i2\pi(\Delta\nu_b + J')/2 - T^{-1} - k \end{bmatrix} \begin{bmatrix} \rho_1 \\ \rho_2 \\ \rho_3 \\ \rho_4 \\ \rho_5 \\ \rho_6 \\ \rho_7 \\ \rho_8 \end{bmatrix} = iC \begin{bmatrix} 1 \\ 1 \\ 1 \\ 1 \\ 1 \\ 1 \\ 1 \\ 1 \end{bmatrix} \quad (12)$$

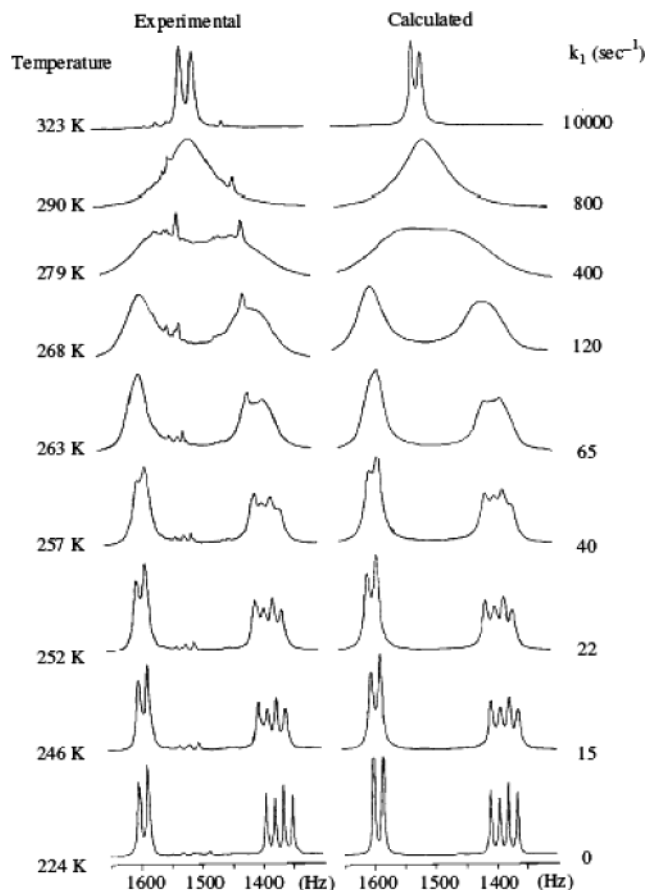


Figure 11. Experimental (left) and calculated (right) ^1H NMR line shapes due to the methylene groups of **10** at different temperatures with derived rate constants.

equations.^{11b}

$$\nu_A - \nu_B = -0.5671T + 368.82, R^2 = 0.9997$$

$$\nu_{A'} - \nu_{B'} = -0.5671T + 339.42, R^2 = 0.9997$$

$$\nu_A - \nu_{A'} = -0.0071T + 31.171, R^2 = 0.8929$$

The line width used for the left-most system was 2.0 Hz, and the right-most system was 1.8 Hz. The value of the coupling constant for former (J) was 14.84 Hz and for the latter (J') 15.11 Hz. Comparisons of observed and calculated ^1H NMR line shapes are shown in Figure 11. The Eyring plot (Figure 12)

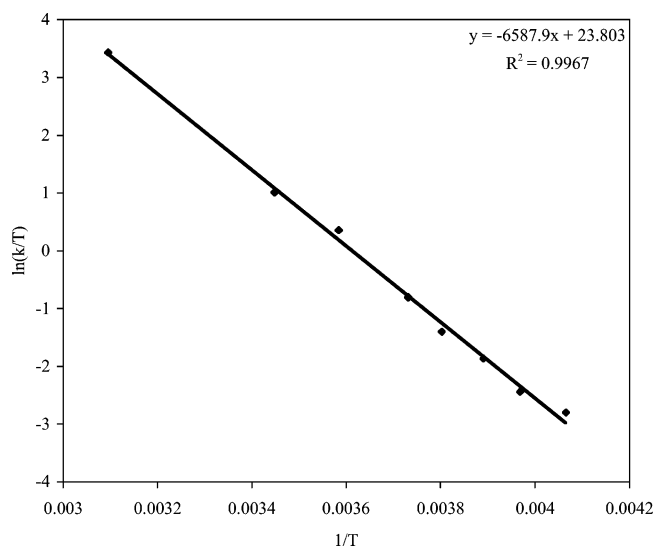


Figure 12. Eyring plot for the inversion in **10** using the methylene resonances in proton line shapes.

then gives the values of ΔH^\ddagger and ΔS^\ddagger as $54.8 \pm 1.3 \text{ kJ mol}^{-1}$ and $0.4 \pm 4.8 \text{ J mol}^{-1} \text{ K}^{-1}$ respectively for the inversion of **10**.

For the case depicted for **11** (Figures 10 and 13), none of the peaks overlap and there are two options to explore: the two outer doublets average and the two inner ones average, or the first and third doublets average and the second and fourth doublets average. However, only the first of these led to reasonable results. The second combination led to an enthalpy of activation of 73.6 kJ mol^{-1} and an entropy of activation of $60.1 \text{ J mol}^{-1} \text{ K}^{-1}$, which seemed unreasonable.

The variation of the shifts with temperature was handled by extrapolation^{11b} as before using the equations

$$\nu_A - \nu_B = -0.7239T + 415.2, R^2 = 0.9968$$

$$\nu_{A'} - \nu_{B'} = -0.5684T + 328.73, R^2 = 0.9959$$

$$\nu_A - \nu_{A'} = -0.1339T + 61.361, R^2 = 0.9879$$

The line width used for the inner two doublets was 3.0 Hz and one for the outer doublets was 3.5 Hz. The values of both of the geminal coupling constants (J and J') were 15.00 Hz. Comparisons of the observed and the calculated ^1H NMR line shapes are shown in Figure 13 and the corresponding Eyring plot, in Figure 14. For this system the values of ΔH^\ddagger and ΔS^\ddagger are $63.2 \pm 2.9 \text{ kJ mol}^{-1}$ and $21.0 \pm 10.3 \text{ J mol}^{-1} \text{ K}^{-1}$ respectively.

Line Shape Analysis of molecule **12** was also attempted, but unfortunately, in this case, the shift of the peaks with temperature did not appear to be linear and a rigorous analysis could not be carried out.

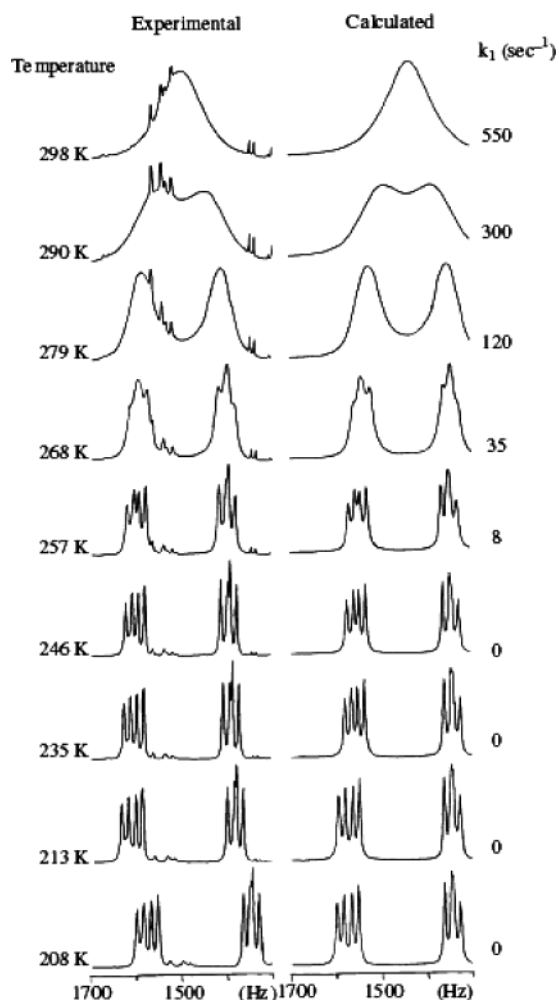
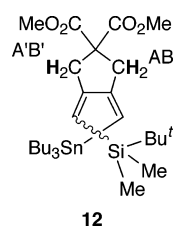


Figure 13. Experimental (left) and calculated (right) ^1H NMR line shapes due to the methylene groups of **11** at different temperatures with derived rate constants.

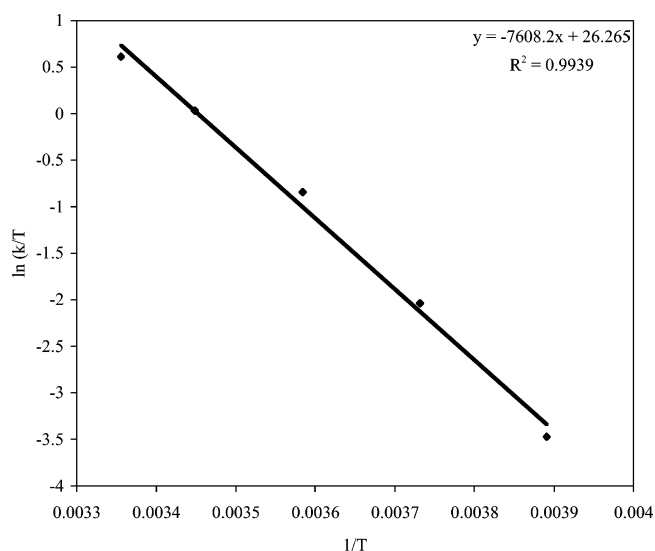


Figure 14. Eyring plot for inversion in **11** using methylene resonances in proton NMR line shapes.

The overall results obtained are summarized in Table 1. For all molecules studied, the free energies of activation are similar ($52\text{--}57 \text{ kJ mol}^{-1}$ at 300 K) and are in the range anticipated from the NMR behavior. It should be noted that the values of

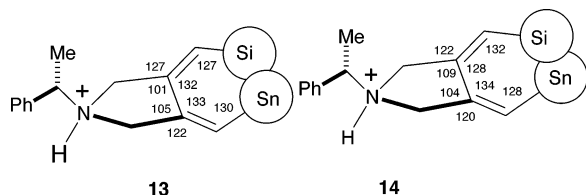


Figure 15. Bond angles of the diastereomeric chiral dienes derived from crystal structure of the amine-oxalate salt (ref. 10).

ΔG^\ddagger and ΔH^\ddagger are more reliable and the values ΔS^\ddagger , prone to error. There is significant change in the enthalpies of activation as the sizes of substituents are changed. For example, in the tri-*n*-butylstannyl derivatives **10** and **11**, there is 8 kJ mol⁻¹ increase in enthalpy of activation in going from a trimethyl- to a triethyl-silyl derivative, reflecting the larger size of the latter. But the entropic contribution brings the overall value of ΔG^\ddagger for the Et₃Si derivative to ~57 kJ mol⁻¹, even though the large error in the entropy estimates should raise some caution. A decrease in the bulk at the C-1 carbon of the cyclopentane (in going from **8** to **9**) leads to a significant decrease in the energy of activation for the helix inversion. This suggests that the cyclopentane ring is involved in the inversion process, as we had suspected from the strikingly broad ¹³C signals in certain temperature regimes. For example, half-width of >400 Hz was observed for the SiMe signals of **8** at 25 °C. Similar features are observed for the ring carbons also (see the Supporting Information for hardcopies of spectra). In general, the overall energies of activation for these series of compounds appear to be lower than would be expected from simple considerations of size of the silicon and tin moieties. This may be a reflection of the significant widening of the Si–C₁–C₂, C₁–C₂–C₃, C₂–C₃–C₄, and C₃–C₄–Sn angles (the numbering of the diene-carbons starting from the Si–C_{sp2} carbon as C₁) of the diene-carbon atoms. The crystal structure determination¹⁰ by X-ray of the related oxalate salts **13** and **14** provide the angles shown in Figure 15. The increased length of the silicon–carbon and tin–carbon bonds, as compared to the C–C bond, could increase or decrease the effective size of the substituents, depending on the relative vectorial orientation of the C–Si and C–Sn bonds. For example, within the diene structure if these bonds are pointed at each other, longer C–Si or C–Sn bonds (*vis-à-vis* C–C bonds) would increase the effective size of these substituents.¹³ On the other hand, the progress toward the transition state results in an orientation where these bonds are pointed away from each other, the longer bonds would decrease the steric congestion. It is interesting to note that compounds **8**, **10**, and **11** have higher energies of activation compared to the somewhat analogous tetramethyl compound **5c** [Z = C(CO₂Et)₂], described by Kiefer¹⁴ ($\Delta G^\ddagger = 46.0$ kJ mol⁻¹ at –46 °C). Another parameter of interest is the bending force constants of C–Si and C–Sn bonds. Unfortunately, the relevant information is not available in the literature.

Even with the admittedly large errors involved in their estimation, the entropies of activation display an interesting behavior, because their values appear to be negative (or a low

positive number) for the triphenylstannane derivatives, but positive (or near zero) for the tributylstannane derivatives. Although it is premature to ascribe any chemical significance to small values of ΔS^\ddagger , it is possible that the transition state is more organized than the ground state for the triphenylstannane derivatives. In these derivatives, it is possible to have correlated or sympathetic motion of the aryl units and the silyl substituents as the crowded transition state for the isomerization is approached. In a series of classical studies, Mislow has described stereochemical consequences of correlated rotations in triarylboranes.¹⁵ With the silyl substituents protruding into the molecular propellers described by the Sn-aryl substituents, the present situation involves more complex motions. However, in this instance it is not unreasonable to expect higher order when the Si and Sn substituents are brought together in the transition state, especially when tin carries phenyl groups. The opposite must be true for the Sn-*n*-butyl derivatives, probably because the *n*-butyl groups have many more degrees of freedom than the phenyl groups, and correlated motions are difficult to envision in this case. Thus, the transition state could be less organized here, leading to a positive entropy of activation. A very significant change (~20 J mol⁻¹K⁻¹) observed in going from Me₃Si to Et₃Si derivative (**10** and **11**) may also support this hypothesis.¹⁶

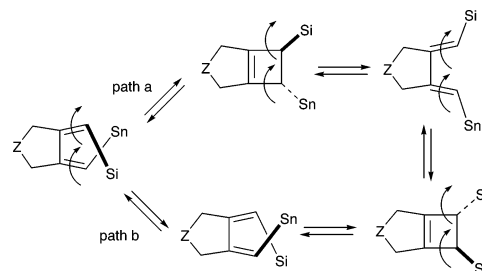
Even though we have not carried out detailed line shape analysis on other 1,2-bisalkylidene cyclopentanes prepared during the synthetic studies,¹⁰ the approximate coalescence (*T_c*) temperature observed during the variable temperature NMR studies clearly provide an indication of the fluxional nature of these molecules. Several examples are included in Table 2. Perhaps the most striking observation is the low *T_c* for the pyrrolidines (–50 to –70 °C). Apparently, with a very low barrier for N-inversion,¹⁷ an alternate mechanism for the conformational reorganization of the cycloalkane is now open.

Ongoing studies in our laboratory include attempts to freeze the helix inversion and explorations of further synthetic applications of these fascinating molecules.

Experimental Section

General. Methylene chloride was distilled from calcium hydride under nitrogen. Benzene and diethyl ether were distilled under nitrogen from sodium/benzophenone ketyl. All of the solvents were freshly

- (15) (a) Mislow, K. *Acc. Chem. Res.* **1976**, *9*, 26. (b) Gust, D.; Mislow, K. *J. Am. Chem. Soc.* **1973**, *95*, 1535. (c) Gust, D.; Mislow, K. *J. Am. Chem. Soc.* **1973**, *95*, 1535. (d) Hummel, J. P.; Gust, D.; Mislow, K. *J. Am. Chem. Soc.* **1974**, *96*, 3679. (e) Blount, J. B.; Finocchiaro, P.; Gust, D.; Mislow, K. *J. Am. Chem. Soc.* **1973**, *95*, 7019.
- (16) An intriguing mechanistic possibility for the helix inversion involves a series of conrotatory electrocyclic ring closures and openings as shown below. However, this remains highly speculative since we have not seen any evidence of the cyclobutene or of the (*EE*)-diene in any of the spectroscopic or chemical experiments.



- (17) Saunders, M.; Yamada, F. *J. Am. Chem. Soc.* **1963**, *85*, 1882.

(13) The effective sizes of groups are different whether they are in a *cis*-1,3-synaxial relationship as in 1,3-cyclohexanes or in the 2,2-positions of a 1,1'-binaphthyl system. In the latter case, the groups are pointed at each other and the interactions increase as the van der Waals radii or the bond lengths increase. See Eliel, E. L.; Wilen, S. H.; Mander, L. N. *Stereochemistry of Organic Compounds*, Wiley: New York, 1994; p. 1144.

(14) Jelinski, L. W.; Kiefer, E. F. *J. Am. Chem. Soc.* **1976**, *98*, 282.

Table 1. Kinetic Parameters Obtained via Line Shape Analysis

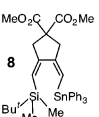
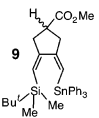
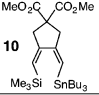
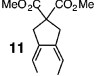
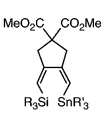
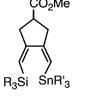
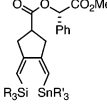
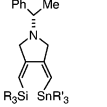
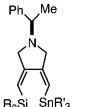
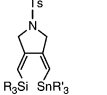
Molecule	ΔH^\ddagger (kJ mol ⁻¹)	ΔS^\ddagger (J mol ⁻¹ K ⁻¹)	ΔG^\ddagger (kJ mol ⁻¹ , 300 K)
	55.4±2.2	-4.3±7.7	56.7±3.2
	48.8±1.1	-11.6±3.8	52.2±1.6
	54.8±1.3	0.4±4.8	54.7±1.9
	63.2±2.9	21.0±10.3	56.9±4.2

Table 2. Coalescence Temperatures of Silylstannyl Dienes^a

Substrate	R'/solvent ^a	R	T _c (°C)
	Bu	Me	10
	Bu	Et	20
	Bu	<i>t</i> -BuMe ₂	20
	Ph	<i>t</i> -BuMe ₂	20
	Ph	<i>i</i> -Pr	-10
	Bu (CD ₂ Cl ₂)	Me	-20
	Bu (CD ₂ Cl ₂)	<i>t</i> -BuMe ₂	-5
	Ph	<i>t</i> -BuMe ₂	0
	Bu	Me	-20
	Ph	<i>t</i> -BuMe ₂	0
	Me (CD ₃ OD)		-50
	Bu (CD ₃ OD)	Me	-60
	Bu (CD ₂ Cl ₂)	<i>t</i> -BuMe ₂	-70
	Ph (CD ₂ Cl ₂)	<i>t</i> -BuMe ₂	-60
	Bu (CD ₂ Cl ₂)	Me	-40
	Ph (CD ₂ Cl ₂)	<i>t</i> -BuMe ₂	-20

^a From 500 MHz ¹H NMR VT NMR in CDCl₃ unless otherwise noted.

distilled or stored over 3 Å molecular sieves. Analytical TLC was done on E. Merck precoated (0.25 mm) silica gel 60 F₂₅₄ plates. Column chromatography was conducted by using silica gel 40 (Natland). HPLC analyses were performed on a Chirasil OD column (25 cm length × 4.6 mm i.d.). Elemental analyses were done by Atlantic Microlab Inc., Norcross, GA.

NMR spectra were obtained in the CDCl₃ solutions (unless otherwise stated) using a Bruker DRX-500 NMR and/or Bruker DPX-400 spectrometers. Chemical shifts are reported in parts per million (ppm, δ) relative to CHCl₃ (δ = 7.240) as an internal standard for proton. Coupling constants are reported in Hertz (Hz). The NMR spectra recorded for line shape analysis required special precautions. The probe

temperature was calibrated using methanol.¹⁸ The shims and tuning were maintained as good as possible at all temperatures. At each temperature, the spectra were recorded 2 to 3 min after the shims had stabilized. The FIDs of the spectra were submitted to Fourier transform and phasing only. No other treatments such as line broadening were performed, as these would affect the shapes of peaks obtained. The calculations of line shape simulations were performed using Mathematica 3.0. Printing of these calculated spectra was done by importing them into Microsoft Excel 2000. The experimental spectra were printed on transparencies, allowing for easy comparison.

Synthesis of Trialkylsilyl-, Trialkyl-, or Triaryl-Stannanes. Trimethylsilyl Tri-*n*-butylstannane. This and other related compounds were prepared according to a procedure described earlier.¹⁹ A solution of 0.8 mL (5.71 mmol) of diisopropylamine in 10 mL of THF was cooled to -78 °C. After 10 min, 2.1 mL (5.00 mmol) of 2.38 M *n*-butyllithium was added over 5 min. After 5 min, the cooling bath was removed and the solution was brought to room temperature. Tri-*n*-butyltin hydride (1 mL, 3.72 mmol) was then added over 5 min. The reaction mixture was stirred at room temperature for 20 min. Trimethylsilyl chloride (0.75 mL, 5.91 mmol) was then added to the solution over minutes. After about 5 min, the solution became cloudy (formation of lithium chloride). The solution was stirred at room temperature for 10 more minutes, evaporated and chromatographed on silica gel (hexanes). The product was obtained in quantitative yield. Alternatively, the product could be distilled at 85°C under 2 mmHg. ¹H NMR (CDCl₃, 400 MHz) δ 0.22 (s, 9 H, SiCH₃), 0.81–0.89 (m, 15 H, CH₂CH₃), 1.24–1.51 (m, 12 H, SnCH₂CH₂). ¹³C NMR (CDCl₃, 125 MHz) δ 1.49 (q), 7.86 (t), 13.74 (q), 27.61 (t), 30.34 (t).

Triethylsilyl Tri-*n*-butylstannane. A solution of 0.5 mL (3.57 mmol) of di-*iso*-propylamine in 5 mL of THF was cooled to -70 °C. After 10 min, 2.5 mL (3.00 mmol) of 1.20 M *n*-butyllithium was added over 5 min. After 15 min, the cooling bath was removed and the solution was brought to room temperature. Tri-*n*-butyltin hydride (0.6 mL, 2.23 mmol) was then added over 5 min. The reaction mixture was stirred at room temperature for 30 min. Triethylsilyl chloride (0.5 mL, 2.98 mmol) was then added to the solution. After about 5 min, the solution became cloudy (formation of lithium chloride). The solution was stirred at room temperature for 3 h, evaporated and chromatographed on silica gel (hexanes). The product was obtained in quantitative yield. ¹H NMR (CDCl₃, 500 MHz): δ 0.72 (6 H, q, 7.9 Hz, SiCH₂), 0.84–0.89 (15 H, m, Bu), 0.97 (9 H, t, 7.9 Hz, SiCH₂CH₃), 1.29 (6 H, sextuplet, 7.4 Hz, Bu), 1.43–1.49 (6 H, m, Bu). ¹³C NMR (CDCl₃, 125 MHz): δ 5.9 (t, SiCH₂), 8.3 (t, Bu), 8.7 (q, SiCH₂CH₃), 13.7 (q, Bu), 27.7 (t, Bu), 30.3 (t, Bu). ¹¹⁹Sn NMR (CDCl₃ 185 MHz): δ -122.8.

***tert*-Butyldimethylsilyl Triphenylstannane.** A solution of 0.5 mL (3.57 mmol) of diisopropylamine in 5 mL of THF was cooled to -78 °C. After 10 min, 2.5 mL (3.00 mmol) of 1.20 M *n*-butyllithium was added over 5 min. After 10 min, the cooling bath was removed and the solution was brought to room temperature. Triphenyltin hydride (0.57 mL, 2.23 mmol) was then added over 5 min. The reaction mixture was stirred at room temperature for 0.5 h. *tert*-Butyldimethylsilyl chloride (600 mg, 3.98 mmol) was then added to the solution. The solution was stirred at room-temperature overnight. The reaction mixture was then evaporated and chromatographed on silica gel (hexanes). The product was obtained 99% yield (1.033 g). ¹H NMR (CDCl₃, 500 MHz): δ 0.40 (6 H, s, SiCH₃), 0.96 (9 H, s, CCH₃), 7.30–7.31 (9 H, m, Ph), 7.50–7.51 (6 H, m, Ph). ¹³C NMR (CDCl₃, 125 MHz): δ -2.5 (SiCH₃), 19.0 (CCH₃), 27.5 (CCH₃), 128.1 (Ph), 128.3 (Ph), 137.5 (Ph), 140.6 (Ph). ¹¹⁹Sn NMR (CDCl₃ 185 MHz): δ -170.8.

Synthesis of Silyl Stannyl Dienes. Di-*O*-methyl-(3*Z*,4*Z*)-3-[(*tert*-butyldimethylsilyl)methylene]-4-[(triphenylstannyl)-methylene]cyclopentane Carboxylate (8). Di-*O*-methylpropargylmalonate (51 mg, 0.245 mmol), (*tert*-butyldimethylsilyl)-triphenylstannane (115 mg, 0.247

(18) Van Geet, A. L. *Anal. Chem.* **1970**, *42*, 679.

(19) Chenard, B. L.; Laganis, E. D.; Davidson, F.; RajanBabu, T. V. *J. Org. Chem.* **1985**, *50*, 3666.

mmol), Pd₂(dba)₃ (7 mg, 0.008 mmol) and *tris*-(pentafluorophenyl)-phosphine (25 mg, 0.047 mmol) were mixed in 0.5 mL of benzene. After 16 h of stirring at room temperature, the solvent was evaporated and the residue was chromatographed on silica gel (hexanes/diethyl ether: 95/5; 80/20) to yield 151 mg (91%) of the desired product. ¹H NMR (CDCl₃, 500 MHz): δ -0.7–0.2 (6 H, brd lump, SiCH₃), 0.78 (9 H, s, SiCCH₃), 3.01 (2 H, broad s, H₂), 3.20 (2 H, broad s, H₃), 3.77 (6 H, s, CH₃), 5.23 (1 H, s, SiCH), 6.13 (1 H, s, J_{Sn-H} = 66.4 Hz, SnCH), 7.39–7.40 (9 H, m, Ph), 7.47–7.70 (6 H, m, Ph). ¹³C NMR (CDCl₃, 125 MHz): δ -5.5–3.5 (lump, SiCH₃), 17.4 (s, SiCCH₃), 26.3 (q, SiCCH₃), 43.8 (t, CH₂), 44.4 (t, CH₂), 52.9 (q, CH₃), 54.7 (s, C₁), 122.4 (d, SnCH), 125.4 (d, SiCH), 128.3 (d, Ph), 128.7 (d, Ph), 137.2 (d, Ph), 139.8 (s, Ph), 155.9 (s), 159.2 (s), 172.0 (s, CO). ¹¹⁹Sn NMR (CDCl₃, 185 MHz): δ -154.5. Assignments were confirmed by COSY, HMQC and DEPT-135. NOE: SnCH → H₅: 5.5%; SnCH → SnPh₃: 3.8%; SiCH → H₂: 4.5%; SiCH → *t*-Bu: 3.8%.

O-Methyl (3Z,4Z)-3-[(*tert*-butyldimethylsilyl)methylene]-4-[(*tri*-phenylstannyl)-methylene]cyclopentane Carboxylate (9). *O*-methyl-2-(2-propynyl)-4-pentynoate (62 mg, 0.413 mmol), *tert*-butyldimethylsilyltriphenylstannane (154 mg, 0.331 mmol), Pd₂(dba)₃ (14 mg, 0.015 mmol) and *tris*-(pentafluorophenyl)phosphine (50 mg, 0.094 mmol) were mixed in 1 mL of benzene. After 15 h at room temperature, the solvent was evaporated and the residue was chromatographed on silica gel (hexanes/diethyl ether 95:5 to 90:10) to get 181 mg (89%) of the desired product. ¹H NMR (CDCl₃, 500 MHz): δ -0.19 (6 H, broad s, SiCH₃), 0.83 (9 H, s, SiCCH₃), 2.68–2.74 (2 H, m, H₂), 2.90 (2 H, d, 7.6 Hz, H₅), 3.06 (1 H, quintet, H₁), 3.77 (3 H, s, CH₃), 5.27 (1 H, s, SiCH), 6.15 (1 H, s, J_{HSn} = 69.5 Hz, SnCH), 7.41–7.43 (9 H, m, Ph), 7.59–7.68 (6 H, m, Ph). ¹³C NMR (CDCl₃, 125 MHz): δ -4.6 (SiCH₃), 17.4 (SiCCH₃), 26.4 (SiCCH₃), 38.3 (C₁), 39.5 (CH₃), 51.8 (CH₃), 121.2 (SnCH), 124.5 (SiCH), 128.3 (Ph), 128.7 (Ph), 137.2 (Ph), 140.0 (Ph), 158.1, 161.2, 175.7 (CO). ¹¹⁹Sn NMR (CDCl₃, 185 MHz): δ -154.5. Assignments were confirmed by COSY and HMQC. NOE: SnCH H₅: 5.4%; SnCH → SnPh₃: 3.4%; SiCH → H₂: 4.4%; SiCH → *t*-Bu: 4.0%.

(3Z,4Z)-Di-O-methyl-3-[(*tri*-*n*-butylstannyl)methylene]-4-[(*tri*-methylsilyl)-methylene]cyclopentanedicarboxylate (10). A solution of 50 mg of di-*O*-methylidipropargylmalonate (0.240 mmol), 83 μL of trimethylsilyltri-*n*-butylstannane (0.239 mmol), 4 mg of Pd₂(dba)₃ (0.004 mmol), 13 mg of *tris*-(pentafluorophenyl)phosphine (0.024 mmol) in 0.2 mL of benzene was prepared. The solution was stirred at room temperature for 22 h. The reaction was then run on silica gel (hexanes/diethyl ether: 9/1) to yield 97 mg (71%) of the desired product. ¹H NMR (CDCl₃, 500 MHz): δ 0.05 (9 H, s, SiCH₃), 0.85–0.88 (15 H, m, Bu), 1.24–1.44 (12 H, m, Bu), 2.66–3.20 (4 H, brd s, H₂, H₅), 3.69 (6 H, s, CH₃), 5.23 (1 H, s, SiCH), 5.65 (1 H, s, J_{HSn} = 50.0 Hz, SnCH). ¹³C NMR (CDCl₃, 125 MHz): δ 0.4 (q, SiCH₃), 10.7 (t, Bu), 13.6 (q, Bu), 27.3 (t, Bu), 28.9 (t, Bu), 44.1 (t), 44.10 (t), 52.7 (q, CH₃), 55.0 (s, C₁), 125.6 (d, SnCH), 126.2 (d, SiCH), 155.3 (s), 155.9 (s), 172.1 (s, CO). The assignment of the ¹³C NMR peaks was confirmed by HMQC. NOE: SnCH → H₂: 4.2%; SnCH → SnBu₃: 4.0%; SiCH → H₅: 4.2%; SiCH → SiMe₃: 2.3%. The retention times on HPLC were: 34.22 min on Chiralsel OJ (100% hexanes, flow of 0.1 mL/min) and 51.92 min on Chiralsel OD (100% hexanes, flow of 0.1 mL/min).

Di-O-methyl-(3Z,4Z)-3-[(*tri*-*n*-butylstannyl)methylene]-4-[(*tri*-ethylsilyl)methylene]-cyclopentanedicarboxylate (11). Di-*O*-methylidipropargylmalonate (51 mg, 0.245 mmol), (triethylsilyl)tri-*n*-butylstannane (99 mg, 0.244 mmol), Pd₂(dba)₃ (7 mg, 0.008 mmol) and *tris*-(pentafluorophenyl) phosphine (22 mg, 0.041 mmol) were mixed in 0.5 mL of benzene. The vial was sealed and placed in an oil bath at 68 °C. After 16 h, the solvent was evaporated and the residue was chromatographed on silica gel (hexanes/diethyl ether: 95/5; 80/20) to yield 51 mg (34%) of the desired product and 17 mg of di-*O*-methylidipropargylmalonate. ¹H NMR (CDCl₃, 500 MHz): δ 0.58 (6 H, q, 7.8 Hz, SiCH₂), 0.85–0.90 (24 H, m, Bu, SiCH₂CH₃), 1.27 (6 H, hex, 7.3 Hz, Bu), 1.37–1.44 (6 H, m, Bu), 2.94 (4 H, broad s, H₃, H₅), 3.69 (6 H, s, CH₃), 5.23 (1 H, s, SiCH), 5.63 (1 H, s, J_{HSn} = 49.5 Hz, SnCH). ¹³C NMR (CDCl₃, 125 MHz): δ 4.5 (t, SiCH₂), 7.4 (q, SiCH₂CH₃), 10.6 (t, Bu), 13.7 (q, Bu), 27.3 (t, Bu), 29.0 (t, Bu), 44.3 (CH₂), 44.4 (CH₂), 52.7 (q, CH₃), 54.9 (s, C₁), 122.3 (d, SiCH), 125.9 (d, SnCH), 155.6 (s), 156.9 (s), 172.2 (s, CO). ¹¹⁹Sn NMR (CDCl₃, 185 MHz): δ -55.0. Assignments were confirmed by COSY, HETCOR and DEPT-135. NOE: SnCH → H₂: 8.8%; SnCH → SnBu₃: 5.5%; SiCH → H₅: 7.7%; SiCH → SiEt₃: 5.7%.

O-Methyl-(3Z,4Z)-3-[(*tert*-butyldimethylsilyl)methylene]-4-[(*tri*-*n*-butylstannyl)-methylene]cyclopentanedicarboxylate. A vial was charged with 200 mg (1.333 mmol) of *O*-methyl-2-(2-propynyl)-4-pentynoate, 540 mg (1.333 mmol) of *tert*-butyldimethylsilyltri-*n*-butylstannane, 30 mg (0.033 mmol) of Pd₂(dba)₃ and 71 mg (0.133 mmol) of *tris*-(pentafluorophenyl)phosphine in 0.4 mL of benzene. The vial was sealed and placed in an oil bath at 52 °C for 17.5 h. The solvent was then evaporated and the residue was chromatographed on silica gel (hexanes/diethyl ether: 99/1) to yield 32 mg (4%) of the desired product. ¹H NMR (CDCl₃, 500 MHz): δ 0.11 (3 H, s, SiCH₃), 0.12 (3 H, s, SiCH₃), 0.90–0.99 (24 H, m, Bu, *t*-Bu), 1.30–1.51 (12 H, m, Bu), 2.66 (4 H, broad s, CH₂), 2.91 (1 H, quintet, 8.3 Hz, H₁), 2.72 (3 H, s, CH₃), 5.34 (1 H, s, SiCH), 5.70 (1 H, s, J_{HSn} = 54.3 Hz, SnCH). ¹³C NMR (CDCl₃, 125 MHz): δ -4.4 (q, SiCH₃), -4.3 (q, SiCH₃), 10.8 (t, Bu), 13.7 (q, Bu), 17.3 (s, SiC), 26.5 (q, SiCCH₃), 27.3 (t, Bu), 29.1 (t, Bu), 38.4 (d, C₁), 39.9 (broad, CH₂), 51.8 (q, COOCH₃), 121.5 (SiCH), 125.1 (SnCH), 176.0 (COO). ¹¹⁹Sn NMR (CDCl₃, 185 MHz): δ -56.5. Assignments were confirmed by COSY, HMQC and DEPT-135. NOE: SnCH → H₅: 4.8%; SnCH → SnBu₃: 4.0%; SiCH → H₂: 3.6%; SiCH → *t*-Bu: 4.0%; SiCH → SiMe₂: 1.0%.

Acknowledgment. We acknowledge the financial assistance by the US National Science Foundation (CHE 0079948 and CHE 0308378) and Petroleum Research Fund of the American Chemical Society (PRF AC 36617).

Supporting Information Available: ¹H, ¹³C, and ¹¹⁹Sn NMR spectra of **8**, **9**, **10**, and **11** including variable temperature spectra, temperature dependence of relevant chemical shifts needed for line shape analysis presented in graphical format (PDF). This material is available free of charge via the Internet at <http://pubs.acs.org>.

JA035136M